Study of transient flow over pyramid roughness in a transitionally rough regime

Mehdi Seddighi

Department of Maritime and Mechanical Engineering
Liverpool John Moores University
James Parson Building, Byrom Street,
Liverpool, L3 3AF, UK
m.seddighi@ljmu.ac.uk

Shuisheng He

Department of Mechanical Engineering
University of Sheffield
Mappin Building, Mappin Street,
Sheffield, S1 3JD, UK
s.he@sheffield.ac.uk

ABSTRACT

We report DNS study of a turbulent-turbulent transient channel flow in transitionally-rough regime. The lower wall of the channel consists of a close-packed pyramid roughness with $k_t/\delta = 0.05$ (where k_t is the roughness height and δ is the channel half-height), and the upper surfaces is smooth. The flow is initially at steady stationary turbulent condition at equivalent roughness heights of $k_s^+ = 14.5$. The flow rate is then suddenly increased to a higher-level and kept at that level until the steady conditions for the final flow are reached. A range of final flow conditions with $k_s^+ = 16.3$ to 41.5 are simulated. The results show that for the cases with final flow condition of $k_{s1}^+ < 30$ the transition process is similar to that of bypass transition for the flow over smooth surface, but with enhanced transition onset depending on the strength of the roughness effect. However, for the cases with $k_{s1}^+ > 30$, the transient flow exhibits a behaviour similar to that of roughness-induced transition. Detailed turbulence statistics and near-wall flow structures are also studied and discussed.

INTRODUCTION

Unsteady flows, in which the bulk velocity, in wall-bounded flows, or free-stream velocity, in boundary layer flows, varies with time, are of general interest since they are frequently encountered in many engineering systems as well as the natural environment. Examples of applications include transient events at a nuclear power plant during various hypothetical fault conditions, turbo-machines, load variations of hydraulic machines, blood flow in large arteries and sediment transport under sea waves. In addition to the practical importance, unsteady flow has some interesting features which share with many other types of flow in fluid dynamics, hence is of great interest on its own. In general, unsteady flows can be divided into two categories: periodic (i.e. pulsating and oscillating flows), and non-periodic flows (i.e. accelerating and decelerating flows), which the latter is the focus of the present study.

For the flow over smooth wall, the classical understanding of the transient wall-bounded flows explains the flow behaviour during the transient period in three stages (Vardy & Brown 2003; He *et al.* 2008, 2011; Ariyaratne *et al.* 2010; Greenblatt & Moss 2004): i) during the first stage (inertial-dominated period) the flow is relaminarised and moved as a "plug-like" flow, ii) new turbulence starts to respond, and iii) the flow quantities approach the quasi-steady values. Despite a well-established observation of the relaminarisation at the early stage of the transient flow, the associated mechanisms are still not well understood. The relaminarisation is also widely observed by the studies on boundary layer flows with FPG (favourable pressure gradient). A well-known salient influence of favourable pressure gradient (FPG), which has been confirmed by many researchers, is stabilisation of the near-wall streaks through damping of the wall-normal and spanwise fluctuations (Blackwelder & Kovasznay 1972; Piomelli *et al.* 2000; Bourassa & Thomas 2009; Piomelli & Yuan 2013.

DNS studies by He & Seddighi (2013, 2015); Seddighi *et al.* (2014) have brought a novel perspective on the transient flow behaviour over smooth surface, showing that, following a flow acceleration from an initially steady *turbulent* flow, the flow undergoes a transient process which exhibits initially a behaviour similar to the laminar flow of the Stokes' first problem, and then transition to turbulent flow much like to bypass transition in a boundary layer (e.g., Jacobs & Durbin 2001). It has been shown that the transient process over the smooth surface can be seen as a new class of bypass transition, in which the pre-existing turbulence of the initial flow to final flow act as the free-stream turbulence (FST) which induces bypass transition senario. The transient behaviour is particularly interesting noting that the initial flow condition is a stationary turbulent shear flow. It has been shown by He & Seddighi (2013) that, for the transient flow following a near-step increase in mass flow rate, the flow within the developing boundary layer undergoes three distinct phases. Initially (pre-transition) the flow is laminar-like and the pre-existing turbulent structures are modulated, resulting in elongated streaks. This leads to a strong and continuous increase in the streamwise velocity fluctuation, but little change in the other two components. The flow then undergoes transition as isolated turbulent spots are generated, which spread and merge with each other. The turbulent spots eventually cover the entire surface of the wall when the flow is fully turbulent. The follow-up studies by Seddighi *et al.* (2014) and He & Seddighi (2015) have shown that a similar transition process occurs for much milder acceleration and and for the flows with various initial and final Reynolds numbers

The behaviour of the transient flow when the final flow condition is near the fully-rough regime was recently studied by Seddighi *et al.* (2015). The equivalent roughness heights of the initial and final flows were, k_s^+= 14.5 and 41.5 respectively, normalised by the wall units. It was shown that the behaviour of the transient flow over the rough wall is characterised by a series of events that resemble those observed in roughness-induced laminar-to-turbulent transitions. Formation and development of standing and counter-rotating hairpin vortex during the transient period were discussed in details.

The present study aims at investigating the transient flow behaviour with various final flow conditions in the transitionally rough regime. Direct Numerical Simulation (DNS) is used to study turbulent-turbulent transient flow behaviour of a channel consists of a close-packed pyramid roughness.

NUMERICAL APPROACHES

DNS is performed using an "in-house" code Seddighi *et al.* (2015). The governing equations are continuity and Navier-Stokes equations which are written in dimensionless form. The equations are normalised using the channel half-height (δ) for length, U_c(centreline laminar Poiseuille velocity) for velocity, and ρU_c^2 for

pressure:

$$\frac{\partial u_i^*}{\partial t^*} + u_j^* \frac{\partial u_i^*}{\partial x_j^*} = -\frac{\partial p^*}{\partial x_i^*} + \frac{1}{Re_c} \frac{\partial^2 u_i^*}{\partial x_j^* \partial x_j^*} + \Pi \qquad (1)$$

$$\frac{\partial u_i^*}{\partial x_i^*} = 0 \qquad (2)$$

The Reynolds number is defined as $Re_c = \frac{\delta U_c}{\nu}$. However, for ease of explanation of the results, unless otherwise stated, the time presented in this paper are rescaled using the bulk velocity of the initial flow (U_{b0}) as the characteristic velocity. Π is the time-mean component of the streamwise pressure gradient to balance the resistance due to friction and form drag (i.e. the value is required to maintain a constant mass flow rate).

A second order central finite difference method is used to discretize the spatial derivatives of the governing equations on a rectangular grid, where a three-dimensional staggered mesh is employed with a non-uniform spacing in the direction normal to the wall. For time advancement, a low storage third-order Runge-Kutta scheme is used for the non-linear terms, and a second order Crank-Nicholson scheme is used for the viscous terms. These schemes are combined with a fractional-step method. The Poisson equation for the pressure is solved by an efficient fast Fourier Transform (FFT). The Message-Passing Interface (MPI) is used to parallelize the code. The channel consists of a smooth top surface and a close-packed pyramid-roughened bottom surface (Figure 1). The roughness is treated using an immersed boundary method (IBM) (Orlandi & Leonardi, 2006). The mesh points, number of roughness elements and computational domain are the same for all simulations: 1024, 32 and 9.6(δ), respectively, in the streamwise direction; 720, 15 and 4.5(δ) in the spanwise direction.

RESULTS AND DISCUSSIONS

The flow is initially at steady stationary conditions. Several initial Reynolds numbers ranging from $Re = 2300$ (with k_s^+=12) to $Re = 4200$ (with k_s^+=21.8) are studied. The flow rate is then rapidly increased to different higher levels, leading to various transitionally-rough upto near fully-rough flow after steady conditions are reached. Figure 1c and Table 1 show the flow condition for the simulations. The initial flow condition is similar to that used in the study of (He & Seddighi, 2013) for a channel with smooth top and bottom surfaces, and Seddighi *et al.* (2015) for a channel with similar roughness to the present study but with the final flow condition close to the fully-rough regime. In addition to the unsteady flow cases, 7 steady flow cases are simulated which fall within transitionally rough regime. Figure 2 shows the roughness function values for the steady flow conditions used in the simulations (Seddighi *et al.*, 2015). The equivalent roughness height, k_s, is obtained to be $k_s = 1.5k_t$ (Seddighi *et al.*, 2015).

Figure 3 shows the development of friction factor for all the transient cases. Also shown in the figure, are the results of He & Seddighi (2013) for the wholly-smooth channel and Seddighi *et al.* (2015) for the transient flow case with final flow condition close to the fully-rough regime.

It is seen that the development of friction factor for R11 is significantly different from that of the smooth-wall case S11 (He & Seddighi, 2013). In contrast with S11, the development shows neither a large initial undershoot, nor a long delay before reaching the corresponding final flow value. Whereas the development

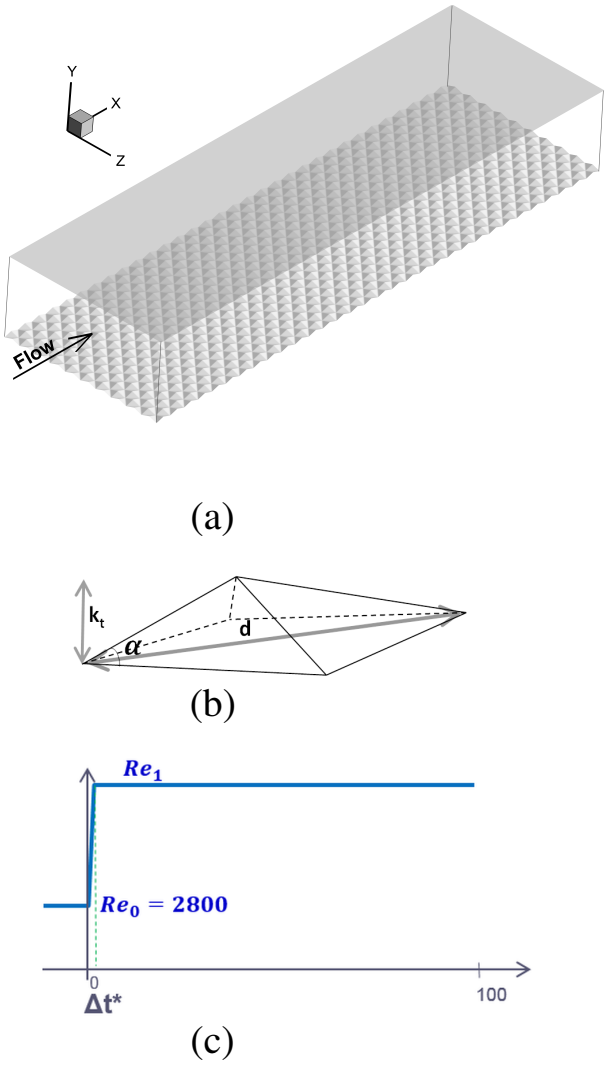

Figure 1. (*a*) Rough-wall roughness structure; (*b*) Geometric parameters for roughness pyramid: $k_t = 0.05(\delta)$, $\lambda = 0.3(\delta)$, $\alpha \approx 18.4°$; (*c*) Flow history for a typical unsteady case.

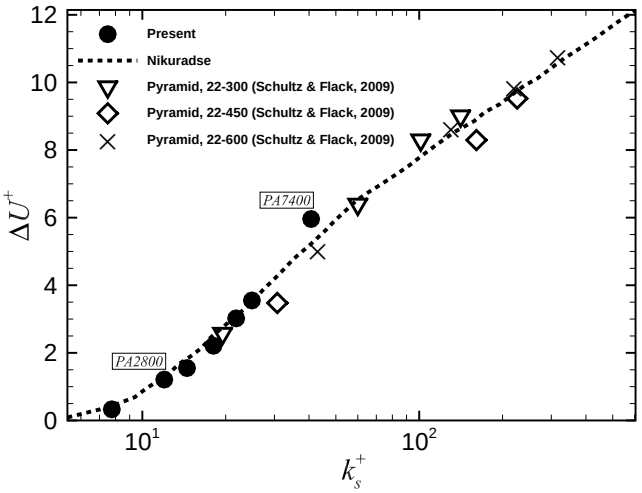

Figure 2. (Roughness function versus equivalent roughness height (Seddighi *et al.*, 2015).

Table 1. Details of the flow cases simulated; the cases R11 and S11 are the same as the cases used by (Seddighi et al, 2015) and (He & Seddighi, 2013), respectively.

Case	Surface	Re_1	Re_1/Re_0	Δt^*	$k_{s_1}^+$
R11	Rough	7400	2.6	0.1	41.5
R12	Rough	6300	2.2	0.07	34.8
R13	Rough	5500	2	0.06	29.2
R14	Rough	4700	1.7	0.04	24.7
R15	Rough	4200	1.5	0.03	21.8
R16	Rough	3800	1.4	0.02	19.6
R17	Rough	3500	1.2	0.02	18.1
R18	Rough	3100	1.1	0.01	16.3
S11	Smooth	7400	2.6	0.1	-

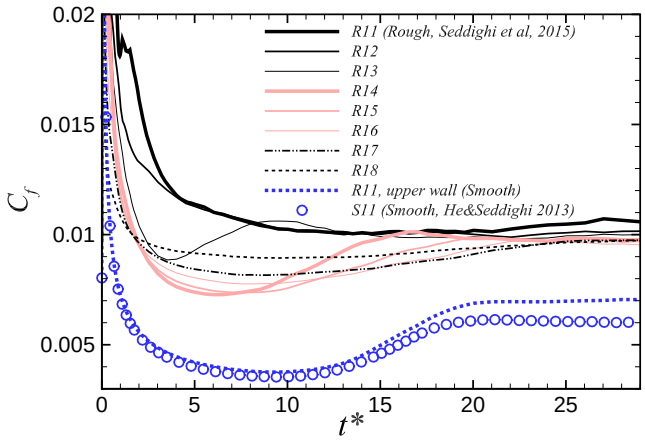

Figure 3. Friction factor for various cases.

of C_f of R12 ($k_{s1}^+ = 34.8$) shows a similar behaviour to R11, rest of the rough cases (all with $k_s^+ < 30$), exhibit a different behaviour to R11: Theses cases show the three-stage behaviour of the transition similar to that of the smooth case, but with an early transition. The development in the first stage (pre-transition) is characterised by elongated turbulence streaks (See figure 5) and the friction factor shows a behaviour which is effectively similar to that of Stokes Solution for the laminar flow. The *pre-transition* is followed by *transition* stage during which isolated turbulence spots are generated and then spread everywhere in the flow, and finally during the *fully-developed* stage turbulence covers whole of the domain. The approximate time that transition occurs is known as critical time, t_{cr} and is considered as the time at which the friction factor reaches its minimum before recovering in the transition stage. The critical time for R18 ($k_{s1}^+ \approx 16.3$) is $t^* \approx 10$. The higher the roughness Reynolds number of the final flow the shorter the critical time are. This is the case for the simulation cases with $k_{s1}^+ < 30$ (R18, R17, R16, R15 and R13). For the cases R11 and R12, however, the development is significantly different and is similar to roughness induced transition. It was discussed by Seddighi *et al.* (2015) that the initial stage of the transition is characterised by the formation of strong primary hairpin vortices (see figure 4) around the roughness and then evolving and subsequently break up of such vortices at later stages of transition.

The different flow structures of iso-surface plot of vortex structures and streamwise streaks for cases R11 and R13, as examples of the cases of roughness-induced and bypass transition, respectively, are shown in Figures 4 and 5. The instants at which the iso-surface plots are shown are close to the transition onset for each case. Different development of the structures is clear from the plots. It is established in (Seddighi *et al.*, 2015) that the development of the counter-rotating vortex is the dominant feature for case R11. It is similar to the roughness-induced laminar-turbulent transition for the boundary layer. For the case R13, however, the instability of the stretched streamwise streaks and formation of isolated turbulence patch is exhibited, which is similar to the bypass-like transition of the turbulent-turbulent transient flow over wholly-smooth wall of He & Seddighi (2013).

Figure 6 shows the development of mean velocity profile for the lower side of the channel, at several instants within the transient period. Here, $y'^+ = (y + \varepsilon_d)^+$, where y is the distance measured from the roughness crest and ε_d is the distance by which the origin is shifted in a way that the log-law is satisfied. The ε_d is considered to be 0.03 for the present results (Seddighi *et al.*, 2015). The development of the mean velocity for R18, R14 and R13 is similar to that report for the smooth surface (He & Seddighi, 2013, 2015; Seddighi *et al.*, 2014). There is a big reduction in the velocity immediately after the excursion of the rapid acceleration and at the very early stages of the transient flow (until $t^* = 0.02$). This is due to forming a high-shear layer in the vicinity of the wall and hence significant increase of the the wall shear stress immediately after the increase of the mass flow rate. The profile then monotonically increases until approximately the onset of transition beyond which it reduces and approaches the final steady flow conditions. The development of the mean velocity profile for R11 shows a similar behaviour to that of the cases with $k_s^+ < 30$ for the sharp decrease at the very early stage of the transient period, but is different for the subsequent stages: The velocity is monotonically increases until reaching the value of steady final flow condition.

Different transition mechanisms can be further examined by studying transport equations for the Reynolds stresses. The production term in the transport equations for the Reynolds stresses are defined as follows:

$$P_{ij} = -\left(\overline{\langle u_i' u_k' \rangle} \frac{\partial \langle \overline{u_j} \rangle}{\partial x_k} + \overline{\langle u_j' u_k' \rangle} \frac{\partial \langle \overline{u_i} \rangle}{\partial x_k} \right) \tag{3}$$

Figures 7 and 8 show a y-z plane, contour plot of the streamwise production (P_{11}) and its various components for R13 and R11, respectively, at an instant around the transition onset. For case R13 (figure 7), the component P_{11y} shows significant contribution to the total production around the crest of the roughness. From equation 3, the P_{11y} consists $\overline{\langle u'v' \rangle}$ and $\frac{\partial \langle \overline{u} \rangle}{\partial y}$ which are also shown in the figure. It is clear that the mean velocity gradient and turbulent shear stress both have significant effect on the total production. For case R11, in addition of the P_{11y}, there is significant contribution from P_{11x} for the region with strong total production. It is interesting to note that the region with strong total production is the location of the primary hairpin vortex at that instant. Consistent with the visualisations of vortex in figure 4, this behaviour shows that the production at the early stage of the transition is generated by the vortex which is formed around the roughness crest and then advected downstream the flow.

CONCLUSIONS

Turbulent-turbulent transient flow of a channel consists of a bottom rough surface and a top smooth surface was studied. The

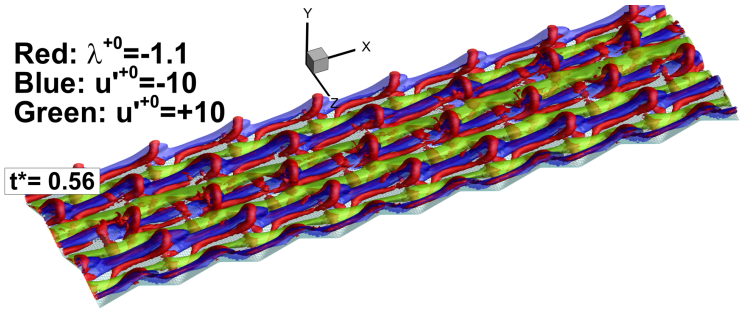

Figure 4. Flow structures in isosurface plots at transition onset for case R11. For clarity, data are shown for one quarter and one fifth in the streamwise and spanwise directions, respectively (Seddighi *et al.*, 2015).

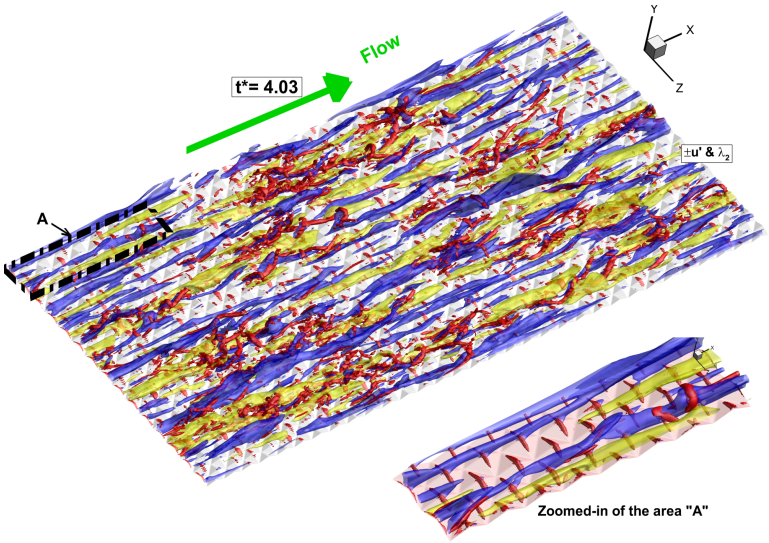

Figure 5. Flow structures in isosurface plots at transition onset for case R13.

roughness was a close-packed rough elements of pyramid shape with a peak-to-trough height of $k_t/\delta = 0.05$. Transient simulations were performed by rapidly increasing the mass flow of a stationary turbulent flow. The time during which the flow reaches the condition of the final steady flow is called transient period and examined in details. All simulations were carried out from an initial steady flow at $Re_0 = 2800$, but the final flow varies in a range from $Re_0 = 3100$ ($k_{s1}^+ > 16.3$) to $Re_0 = 7400$ ($k_{s1}^+ = 41.5$). The behaviour of the flow in the early stage of the transient flow over the rough wall studied, differs strongly depending on the final flow condition. For the cases with the final flow condition of $k_s^+ > 30$, a roughness-induced transition is exhibited. The transition resembles roughness-induced transition of the boundary layer flow. However, when the equivalent roughness height of the final flow is below 30, a bypass-like transition occurs which is similar to the flow over a smooth wall (He & Seddighi, 2013), but with enhanced transition.

ACKNOWLEDGMENTS

The authors are grateful to the UK Engineering and Physical Science Research Council (EP/G068925/1) to provide financial support for this study. The work made use of the facilities of the N8 HPC (EP/K000225/1), and the UK National Supercomputer ARCHER sponsored by EPSRC through the UK Turbulence Consortium (EP/L000261/1).

REFERENCES

Ariyaratne, C., He, S. & Vardy, A. E. 2010 Wall friction and turbulence dynamics in decelerating pipe flows. *Journal of Hydraulic Research* **48(6)**, 810–821.

Blackwelder, Ron F. & Kovasznay, Leslie S. G. 1972 Large-scale motion of a turbulent boundary layer during relaminarization. *Journal of Fluid Mechanics* **53** (01), 61–83.

Bourassa, C. & Thomas, F. O. 2009 An experimental investigation of a highly accelerated turbulent boundary layer. *Journal of Fluid Mechanics* **634**, 359–404.

Greenblatt, D. & Moss, E. A. 2004 Rapid temporal acceleration of a turbulent pipe flow. *Journal of Fluid Mechanics* **514**, 65–75.

He, S., Ariyaratne, C. & Vardy, A. E. 2008 A computational study of wall friction and turbulence dynamics in accelerating pipe flows. *Computers and Fluids* **37** (6), 674–689.

He, S., Ariyaratne, C. & Vardy, A. E. 2011 Wall shear stress in accelerating turbulent pipe flow. *Journal of Fluid Mechanics* **685**, 440–460.

He, S. & Seddighi, M. 2013 Turbulence in transient channel flow. *Journal of Fluid Mechanics* **715**, 60–102.

He, S. & Seddighi, M. 2015 Transition of transient channel flow after a change in Reynolds number. *Journal of Fluid Mechanics* **764**, 395–427.

Jacobs, R. G. & Durbin, P. A. 2001 Simulations of bypass transition. *Journal of Fluid Mechanics* **428** (1), 185–212.

Orlandi, P. & Leonardi, S. 2006 DNS of turbulent channel flows with two- and three-dimensional roughness. *Journal of Turbulence* **7**, 1–22.

Piomelli, U., Balaras, E. & Pascarelli, A. 2000 Turbulent structures in accelerating boundary layers. *Journal of Turbulence* **1**, 1–16.

Piomelli, U. & Yuan, J. 2013 Numerical simulations of spa-

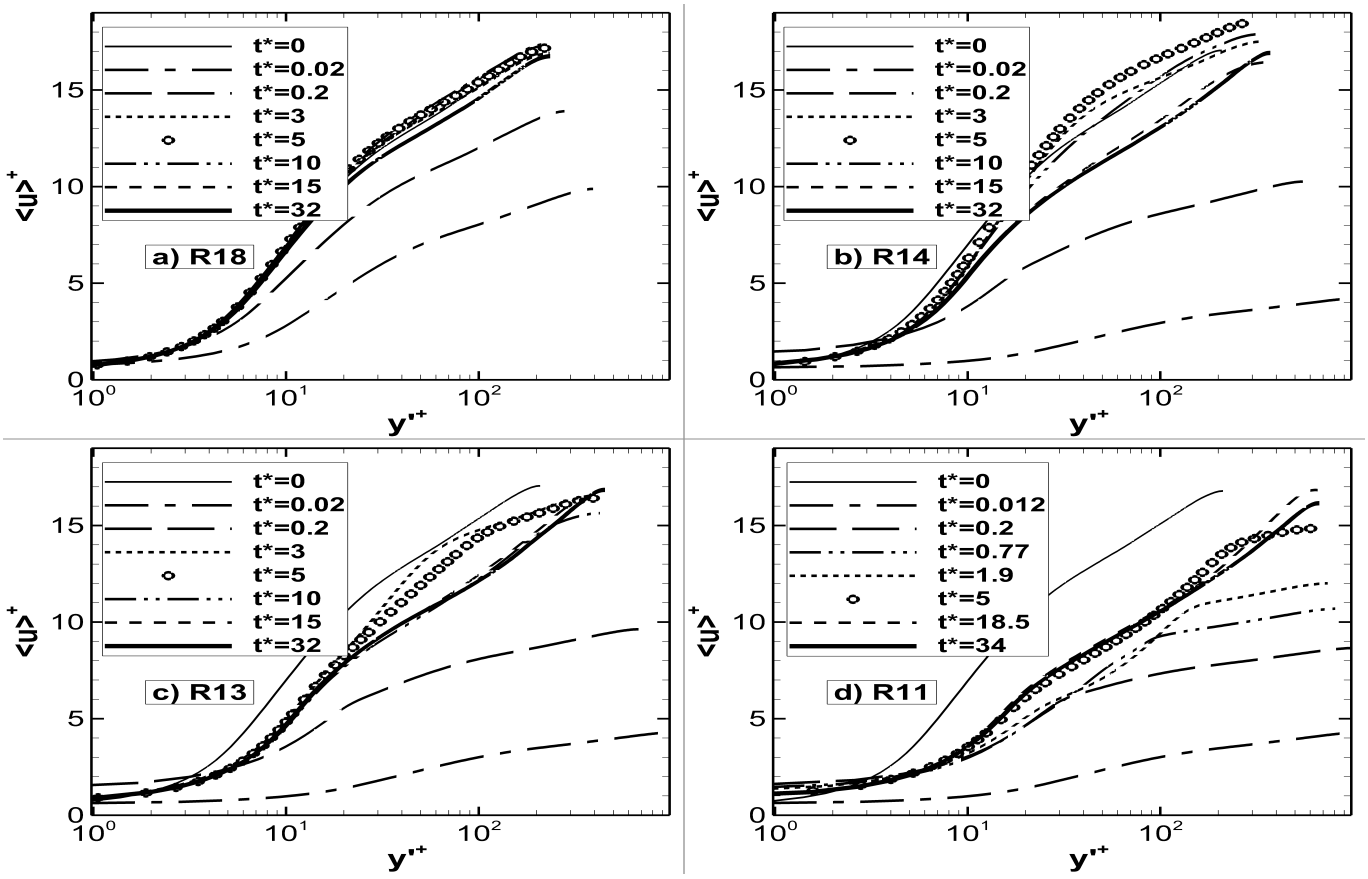

Figure 6. Development of mean velocity profiles at several instants.

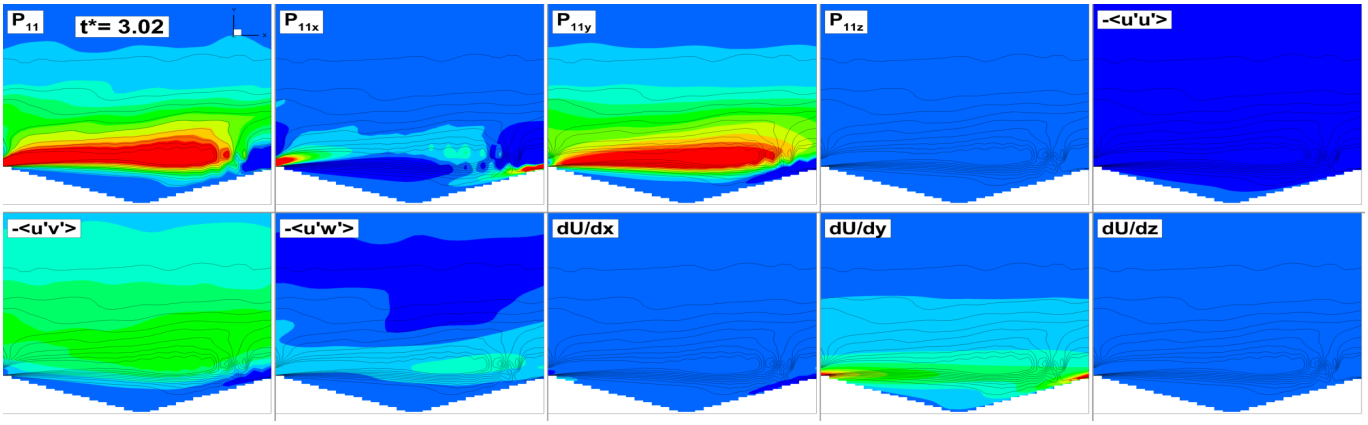

Figure 7. Plot of contour lines of turbulent shear stress of case R13, $\overline{u'v'}$, shaed by streamwise turbulent shear stress production, P_{11}, and its various components, for a y-z plane at $\frac{x}{\lambda} = 0$.

tially developing, accelerating boundary layers. *Physics of Fluids* **25** (10), 101304.

Seddighi, M., He, S., Pokrajac, D., O'Donoghue, T. & Vardy, A. E. 2015 Turbulence in a transient channel flow with a wall of pyramid roughness. *Journal of Fluid Mechanics* **781**, 226–260.

Seddighi, M., He, S., Vardy, A. E. & Orlandi, P. 2014 Direct numerical simulation of an accelerating channel flow. *Flow, Turbulence and Combustion* **92**, 473–502.

Vardy, A. E. & Brown, J. M. B. 2003 Transient turbulent friction in smooth pipe flows. *Journal of Sound and Vibration* **259 (5)**, 1011–1036.

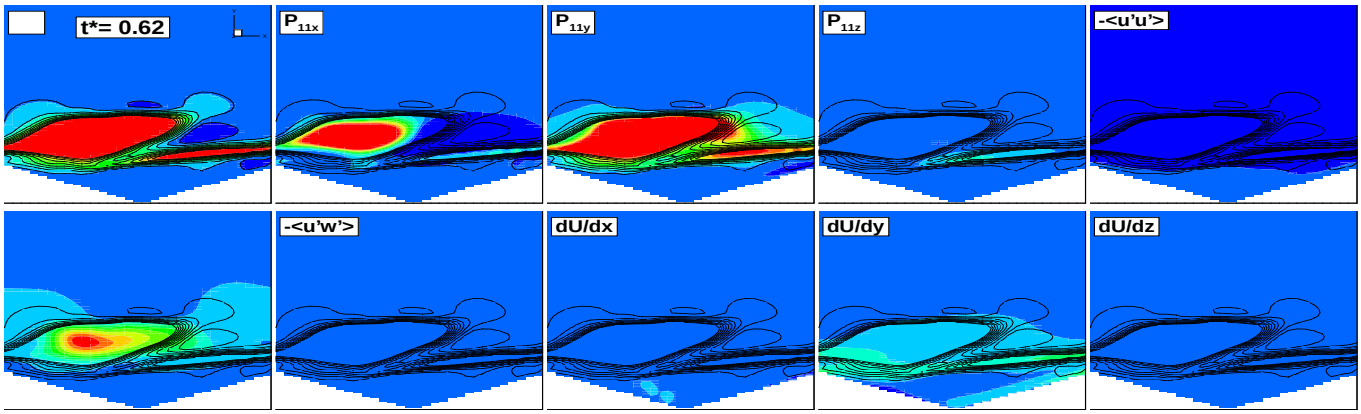

Figure 8. Plot of contour lines of turbulent shear stress of case R11, $\overline{u'v'}$, shaed by streamwise turbulent shear stress production, P_{11}, and its various components, for a y-z plane at $\frac{x}{\lambda} = 0$.